2010 IEEE International Conference on Robotics and Automation
Anchorage Convention District
May 3-8, 2010, Anchorage, Alaska, USA

Enhanced Trajectory Tracking Control with Active Lower Bounded Stiffness Control for Cable Robot

Kun Yu, Leng-Feng Lee, Chin Pei Tang, and Venkat N. Krovi

Abstract— **Cable robots have seen considerable recent interest ensuing from their ability to combine a large workspace with significant payload capacity. However, the cables can apply forces to the end-effector only when they are in tension, and thus form a subclass of control problems requiring unilateral control inputs. Furthermore, actuation redundancy occurs when surplus cables are introduced within the system. On one hand, such redundancy needs to be carefully resolved for accurate tracking of the task. On the other hand, it allows the redistribution of the actuation forces to satisfy some secondary criteria. In this paper, we apply such redundancy for enhanced trajectory tracking by actively controlling the task stiffness of the end-effector. The scheme allow us to specify a lower bound of the task stiffness, which is intended to provide improved trajectory tracking and disturbance rejection performance. Finally, we illustrate the improved control performance within a virtual prototype co-simulation framework.**

I. Introduction

CABLE ROBOTS are formed by replacing the multiple sets of articulated links within a parallel manipulator with cables. This allows various motion trajectories at the end-effector to be created by coordinated extension or retraction of the cables within the system. However, the cables can apply forces to the end-effector only when they are in tension. Thus, they form a subclass of the set of control problems requiring unilateral control inputs. In addition, when more cables than the required degree-of-freedom (DOF) of the task are introduced, a redundant system is created and requires suitable resolution scheme in order to properly track the desired task [1]. On one hand, this creates indeterminacy in terms of the force distribution required to achieve the desired end-effector motion. On the other hand, without careful coordination, substantial internal forces can build up within the closed-loop system, which can potentially damage to the system. Thus, effective resolution scheme for such actuation redundancy is critical to ensure accurate yet robust task execution.

Suitable development of actuation redundancy resolution schemes can not only allow better (primary) trajectory tracking performance but also allow the redistribution of the actuation forces to satisfy secondary criteria. For instance, from a parallel manipulator perspective, redundancy resolution methods have proved useful in eliminating singularities within workspace [2], reducing the chance of system failure, realizing optimal actuation distribution and power consumption [3], and enabling active stiffness control for modulating internal actuation distribution [1, 4].

Stiffness is an important characteristic that is directly related to the rigidity of a robotic structure, the robot's performance of trajectory tracking, and the robot's capability for disturbance rejection [5-6]. In the task space, it relates the tracking error to external force exerted by the end-effector. A class of control method called stiffness control (or more generally impedance control) seeks to track or regulate such stiffness in order to achieve better control performance. In [4], such stiffness control method was developed to achieve desired end-effector stiffness using redundant actuation for general rigid robotic manipulators.

While redundantly actuated parallel robots have been treated extensively in the past, the problem of the unilateral nature of the cable tension constraint is challenging. However, many parallels exist between such requirement with the unilateral normal force constraints arising in the context of multi-fingered hands and multi-legged walkers [7]. Several approaches, including the feedback linearization [8] and time optimal control [9], were proposed to resolve redundancy under unilateral actuation.

However, to our knowledge, the application of stiffness control method for redundantly actuated cable robots with the unilateral actuation constraints has not been explored. In this paper, we formulate the redundancy resolution scheme using the active stiffness control method for cable robot. We apply such redundancy for enhanced trajectory tracking by way of introducing a lower bound task stiffness within the control scheme. Such bounding is intended to provide minimal guarantees of trajectory tracking and disturbance rejection performance. Finally, we illustrate the improved control performance within a virtual prototype co-simulation framework.

The rest of the paper is organized as follows: Section II presents the modeling and the feedback linearization control method for a cable robot. Section III then explores the resolution scheme to take into account for the redundant actuation within the robot. Section IV introduces the proposed active stiffness control scheme with LBSC in detailed, and Section V presents the case studies to illustrate the effectiveness of the method. We conclude the paper in Section V.

This work was supported in part by the NSF Awards IIS-0347653 (CAREER) and CNS-0751132, and the UT Dallas Research Fund.

K. Yu is with Cameron Compression Systems, Buffalo NY 14227, USA. Email: kun723.yu@gmail.com.

L.-F. Lee and V. N. Krovi are with Department of Mechanical and Aerospace Engineering, SUNY at Buffalo, Buffalo NY 14260, USA. Emails: {llee3,vkrovi}@buffalo.edu.

C. P. Tang is with School of Engineering and Computer Science, UT Dallas, Richardson TX 75080, USA. Email: chinpei@ieee.org.

II. Modeling and Control of Cable Robot

A. Kinematic and Dynamic Modeling

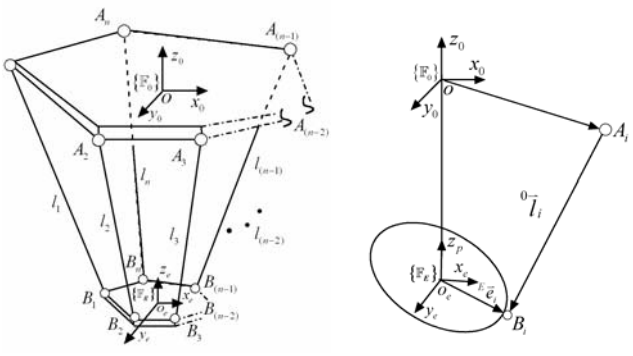

(a) (b)

Fig. 1. (a) Schematic of the spatial cable robot under consideration, and (b) sketch of cable *i* and its related position vector.

As shown in Figure 1, the spatial cable robot under consideration consists of an upper fixed plate and a lower moving end-effector plate actuated by the tension forces created by extending and retracting the n cables connected between the plates. Following [8], the connection points of the cables at the upper and lower plates are respectively labeled as A_i and B_i, for i = 1, 2, $\cdots$ n, and frames $\{\mathbb{F}_0\}$ and $\{\mathbb{F}_E\}$ are respectively rigidly fixed at the centers of the polygon formed by the vertices A_i and B_i. Assuming that the cables are always in tension, let l_i be the length, $\dot{l}_i$ be the extending/retracting rate, ${}^0\vec{l}_i$ be the position vector, and $\hat{l}_i = {}^0\vec{l}_i / \| {}^0\vec{l}_i \|$ be the unit vector of the i th cable. Defining ${}^E\vec{e}_i$ be the position vector with respect to frame $\{\mathbb{F}_E\}$ of the cable connection in the lower plate, ${}^0\vec{e}_i$ be the position vector with respect to frame $\{\mathbb{F}_0\}$ of the cable connection in the upper plate, ${}^0R_E$ is the rotation matrix from frame $\{\mathbb{F}_0\}$ to $\{\mathbb{F}_E\}$, and taking into account for the closed kinematic loops formed, the kinematics of the system can be derived as:

$$\dot{l} = J\dot{X} \tag{1}$$

where

$$J = \begin{bmatrix} \hat{l}_1^T & \left({}^0\vec{e}_1 \times \hat{l}_1\right)^T \\ \vdots & \vdots \\ \hat{l}_n^T & \left({}^0\vec{e}_3 \times \hat{l}_3\right)^T \end{bmatrix} = \begin{bmatrix} \hat{l}_1^T & -\left(\hat{l}_1 \times {}^0R_E\,{}^E\vec{e}_1\right)^T \\ \vdots & \vdots \\ \hat{l}_n^T & -\left(\hat{l}_n \times {}^0R_E\,{}^E\vec{e}_n\right)^T \end{bmatrix}$$

$\dot{l}^T = \begin{bmatrix} \dot{l}_1 & \cdots & \dot{l}_n \end{bmatrix}$ is the cable velocity vector and $\dot{X}^T = \begin{bmatrix} \dot{x} & \dot{y} & \dot{z} & \omega_x & \omega_y & \omega_z \end{bmatrix}$ is the end-effector velocity with respect to the fixed plate.

Finally, assuming that the cables are massless, the dynamic equation can be derived using Newton-Euler method as:

$$\begin{bmatrix} m\ddot{x} \\ m\ddot{y} \\ m\ddot{z} \\ I_m \begin{bmatrix} \dot{\omega}_x \\ \dot{\omega}_y \\ \dot{\omega}_z \end{bmatrix} + \begin{bmatrix} \omega_x \\ \omega_y \\ \omega_z \end{bmatrix} \times I_m \begin{bmatrix} \omega_x \\ \omega_y \\ \omega_z \end{bmatrix} \end{bmatrix} = -J^T \begin{bmatrix} F_1 \\ F_2 \\ \vdots \\ F_n \end{bmatrix} \tag{2}$$

where m and I_m are respectively the mass and the moment of inertia of the lower plate. The general (task space) dynamic can then be written as the following form:

$$M(X)\ddot{X} + h\left(X, \dot{X}\right)\dot{X} + g(X) = -J^T F \tag{3}$$

where M, h, g, $F \geq 0$ are respectively inertial matrix, Coriolis/centrifugal matrix, gravitational forces and tension forces of the cables.

B. Feedback Linearization

The trajectory tracking for system (3) can be achieved by using the feedback linearization method [8]. Define the error between the desired task trajectory $X_d(t)$ and actual task trajectory $X(t)$ be $e(t) = X_d(t) - X(t)$. Choosing the feedback law of the form:

$$-J^T F = h\dot{X} + g + M\left(\ddot{X}_d - K_p e - K_d \dot{e}\right) \tag{4}$$

where K_p and K_d are respectively the positive diagonal PD gain matrices. The task space error dynamics can then be solved, by substituting (4) into (3), as:

$$\ddot{e} + K_p e + K_d \dot{e} = 0 \tag{5}$$

which shows that X will asymptotically track X_d.

III. Redundancy Resolution

In this section, we formulate an effective actuation redundancy resolution scheme based on the generalized pseudo-inverse method. Given an n dimensional cable actuation and m ($\leq n$) dimensional task, from (4), let:

$$W_{m\times 1} = S_{m\times n} F_{n\times 1},\ S_{m\times n} = -J^T_{m\times n} \tag{6}$$

The linear equation can generally be solved by the pseudo-inverse method as:

$$F = S^{\#}W + \left(I - S^{\#}S\right)\vec{z} \tag{7}$$

where I is an $n\times n$ identity matrix, $\vec{z}$ is an arbitrary n vector, and $S^{\#} = S^T\left(SS^T\right)^{-1}$ is Moore-Penrose pseudo-inverse of S. The solution in (7) consists of two terms: the first term $F_p = S^{\#}W$ is the particular solution to (6), which corresponds to its minimum norm solution in the least squares sense; and, the second term $F_h = \left(I - S^{\#}S\right)\vec{z}$ is the homogeneous (null space) solution to Eq. (6). In [10-11], F_p is interpreted as the required equilibrating force that causes the effective motion of the system, but F_h is internal force that does not contribute the effective work to the system. In general, in the control of cable robot, the

positivity of the particular solution cannot be guaranteed, which can cause the input force F to violate the unilateral tension constraint. Hence, we can take the advantage of the additional homogeneous term (which can take on any arbitrary value due to the redundancy) to maintain the positivity of the input force F. Effectively, we are *modulating and redistributing the internal forces within the redundant system* so that the positivity of the input forces to the system is ensured.

A. Parameterization of Null Space

Consider the null space matrix $\hat{S} = I - S^{\#}S$ in (7), which generally has rank $n-m \le n$. This implies that only $n-m$ independent vectors are required to parameterize the null space. During the computation of $\hat{S}$, arbitrary switching of the $n-m$ columns may cause discontinuity of F_h [12]. To solve this problem, we can make use of the singular value decomposition of $\hat{S}$ to take advantage of its unique basis vector arrangement. Decompose $\hat{S}$ into $U\Delta V^T$, where the matrices U and V are respectively formed by the normalized eigenvectors of $\hat{S}\hat{S}^T$ and $\hat{S}^T\hat{S}$, and the matrix Δ consists of the singular values of $\hat{S}$ along its diagonal in the descending order. The new null space matrix can then be formed by choosing the first $n-m$ columns of U, where $N(S) = \begin{bmatrix} u_1 & u_2 & \cdots & u_{n-m} \end{bmatrix}$. Hence, (7) can be rewritten using this new parameterization as:

$$F = S^{\#}W + \sum_{k=1}^{n-m} \alpha_k N_k = F_p + N(S)\bar{\alpha} \tag{8}$$

where $\bar{\alpha}^T = \begin{bmatrix} \alpha_1 & \alpha_2 & \cdots & \alpha_{n-m} \end{bmatrix}$ is the new arbitrary vector.

B. Resolution by Tension Force Optimization

Since the vector $\bar{\alpha}$ in (8) is arbitrary, we can take advantage of these free variables to optimize the tensions among the cables, which can be formulated as a linear programming problem:

$$\min_{\bar{\alpha}}: \qquad \beta_f{}^T \bar{\alpha} \tag{9}$$

$$subject\ to: \qquad -N(S)\bar{\alpha} \le F_p \tag{10}$$

where F is defined in (8), β_f are vector of weights, and the inequality constraint in (10) is intended to maintain the positivity of cable input F.

IV. Active Stiffness Control

A. Task Stiffness of Cable Robot

Consider the force system at the end-effector $W^T = \begin{bmatrix} f & m \end{bmatrix}$, the incremental displacement of the end-effector δX caused by the incremental force δW can be related by a stiffness matrix K_X as:

$$\delta W = K_X \delta X \tag{11}$$

where K_X is called the *task or Cartesian stiffness matrix*. Similarly, the incremental tension forces exerted by the cables δF and the incremental displacement within the cables δl caused by the tension forces can be related as:

$$\delta F = K_l \delta l \tag{12}$$

where K_l the joint space stiffness matrix, which is simply the diagonal matrix with entries of the stiffness of each cable. Differentiating (6), we get:

$$dW = (dS)F + S(dF) \tag{13}$$

Substituting, (11) and (12) into (13) yield:

$$K_X dX = (dS)F + SK_l dl \tag{14}$$

Note carefully that dS is the differential of the matrix S, which can be computed as:

$$dS = \sum_{j=1}^{m} \frac{\partial S}{\partial X_j} dX_j \tag{15}$$

In addition, noting from (1) that $dl = JdX$, canceling the common dX term in (14) yield:

$$K_X = K_g + K_c \tag{16}$$

where

$$K_g = \begin{bmatrix} \dfrac{\partial S}{\partial X_1}F & \dfrac{\partial S}{\partial X_2}F & \cdots & \dfrac{\partial S}{\partial X_6}F \end{bmatrix} \tag{17}$$

$$K_c = SK_l J = -J^T K_l J \tag{18}$$

Chen and Kao [13] termed this mapping as Conservative Congruence Transformation (CCT). It is important to note from this transformation that the task stiffness not only depends on the cable stiffness in the term K_c, the internal cable actuation force F in the term K_g can also significantly contribute to the overall task stiffness. Hence, in what follows, we modulate this required tension force such that some specific task stiffness can be achieved.

Defining the tensor operator:

$$H = \begin{bmatrix} \dfrac{\partial S}{\partial X_1} & \vdots & \dfrac{\partial S}{\partial X_2} & \vdots & \cdots & \vdots & \dfrac{\partial S}{\partial X_m} \end{bmatrix}^T_{m\times(m\times n)} \tag{19}$$

and substituting (8) into (17) yields:

$$\begin{aligned} K_g &= HF = H\left[F_p + N(S)\bar{\alpha}\right] \\ &= HF_p + HN(S)\bar{\alpha} \end{aligned} \tag{20}$$

The overall task stiffness (16) can then be written as:

$$K_X = \left\{HF_p + H\left[N(S)\bar{\alpha}\right]\right\} - \left\{J^T K_l J\right\} \tag{21}$$

Hence, one way to resolve the actuation redundancy in the system is to add the requirement of a desired overall task stiffness K_X^d. The tension force optimization problem in (9) and (10) can then be augmented using an equality constraint as:

$$\min_{\bar{\alpha}}: \qquad \beta_f^T \bar{\alpha} \tag{22}$$

$$subject\ to: \left\{HF_p + H\left[N(S)\bar{\alpha}\right]\right\} - \left\{J^T K_l J\right\} = K_X^d \tag{23}$$

$$-N(S)\bar{\alpha} \le F_p \tag{24}$$

The computational issue for (23) is addressed in [14].

However, this scheme can be greatly limiting when the

number of extra cables is less than the independent components of desired stiffness matrix. Furthermore, realistically, it is not desirable to introduce too many extra cables as it increases the probability of cable interference and greatly limits its workspace. In addition, the feasible solution may not always exist, i.e. the desired stiffness cannot be achieved in most designs under the strict criteria. We noted some of these limitations in our previous work [15], and, hence, we improve the control scheme by relaxing this criteria as discussed subsequently.

B. *Lower Bound Stiffness Control (LBSC)*

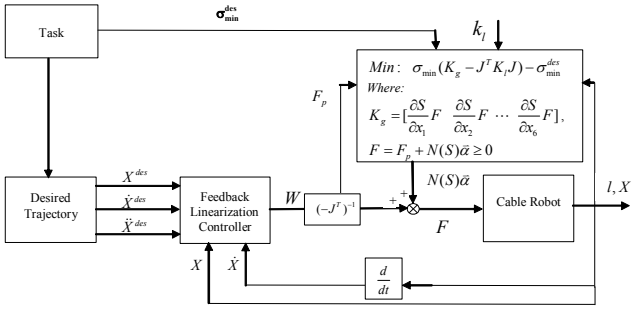

Fig. 2. Block diagram of Lower Bound Stiffness Control for the cable robot.

In Lower Bound Stiffness Control (LBSC), instead of specifying a strict desired value for all components of the task stiffness, we relax the requirement by just specifying a lower bound for the stiffness. The task stiffness matrix is a positive semi-definite symmetric matrix, where the eigenvalues are the values of the stiffness of the corresponding principal directions given by the corresponding eigenvectors. Hence, in the formulation, we can make sure the smallest eigenvalue $\sigma_{\min}$ to be greater than the minimum value of $\sigma_{\min}^{d}$. Specifically, from (21), the objective function to be minimized can be defined by:

$$\begin{aligned} f &= \sigma_{\min}\left(K_X\right) - \sigma_{\min}^{d} \\ &= \sigma_{\min}\left(\left\{HF_p + H\left[N(S)\bar{\alpha}\right]\right\} - \left\{J^T K_l J\right\}\right) - \sigma_{\min}^{d} \end{aligned} \tag{25}$$

The overall LBSC scheme is shown in the block diagram form in Fig. 2. k_l is first prescribed as the stiffness constant of each cable. In each iteration, we solve for the cable control input forces as an optimization problem with explicit design variable $\bar{\alpha}$ to minimize the objective function (25) under the positive cable input forces F constraint (10). Then the simultaneous position and velocity information of the cable robot is provided to the feedback linearization controller and the task space control output is generated. This output is then filtered through the inverse dynamics operator $\left(-J^T\right)^{-1}$ to calculate the particular solution and the homogenous solution of the new cable control input force candidates in terms of the design variables in $\bar{\alpha}$. $\bar{\alpha}$ is then optimized by a optimizer and used to compute the new cable control input forces F.

V. Simulation Framework and Case Studies

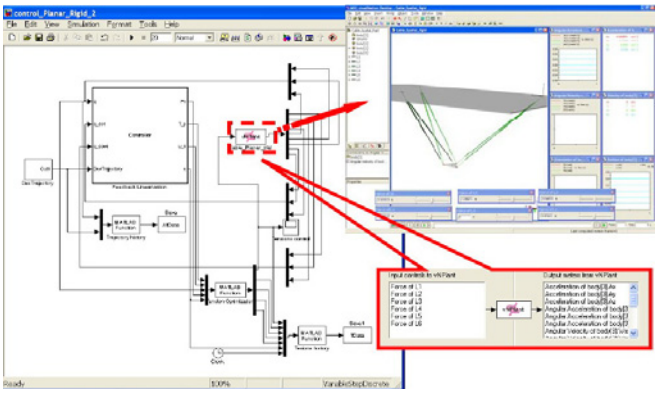

Fig. 3. MATLAB/Simulink/MSC visualNastran co-simulation framework.

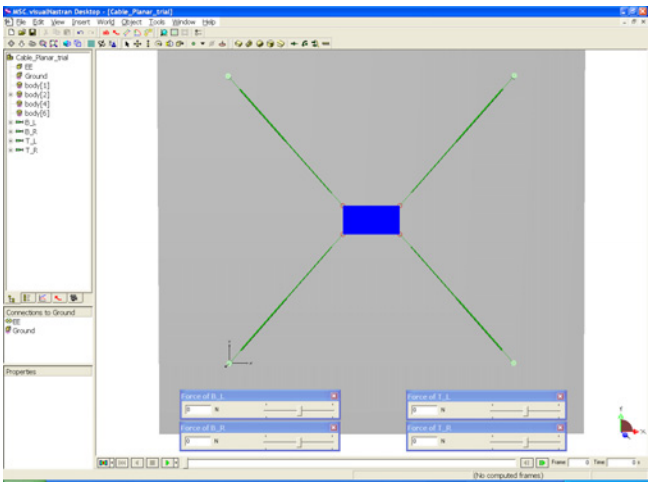

Fig. 4. The configuration of the planar cable robot with rigid-body end-effector under consideration modeled in MSC visualNastran.

We evaluate the proposed redundancy resolution and control method in a virtual prototype co-simulation framework using MATLAB/Simulink/MSC visualNastran as shown in Fig. 3. Such implementation is also intended to form the basis of real-time hardware-in-the-loop co-simulation with a physical prototype - see [14] for details. Several case studies were performed including both planar and spatial cases with point-mass and rigid-body end-effector.

In this paper, we present the results with planar 4-cable robot system manipulating a rigid-body end-effector for (a) trajectory tracking with/without LBSC, and (b) disturbance rejection with/without LBSC. The planar rigid-body end-effector, shown in Fig. 4, is modeled as a rigid plate attached to four cables in a plane and actuated independently by four motors. The four motors forming the base are located at (0, 0) m, (1, 0) m, (1, 1) m and (0, 1) m. Since the end-effector has three task space DOF x, y, ϕ but is driven by four actuated cables, it has degree of redundancy of one. In all case studies, the trajectory traced is a straight line with $x = 0.55\ m$, $y = (0.5 + 0.1t)\ m$, and $\phi = 0\ rad$ at desired velocity of $0.1\ m/s$, and it is initially placed with an error at $(0.5,\ 0.5)\ m$, $\phi = 0\ rad$.

A. Trajectory Tracking with/without LBSC

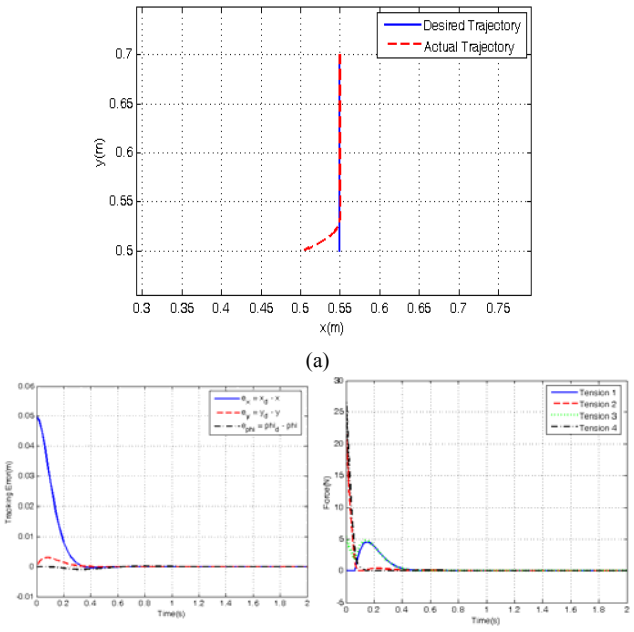

(a) (b) (c)

Fig. 6. Trajectory tracking performance without LBSC: (a) the desired and actual tracking trajectories; (b) the tracking errors of x, y, ϕ; and (c) the tension force in all the cables during the trajectory tracking.

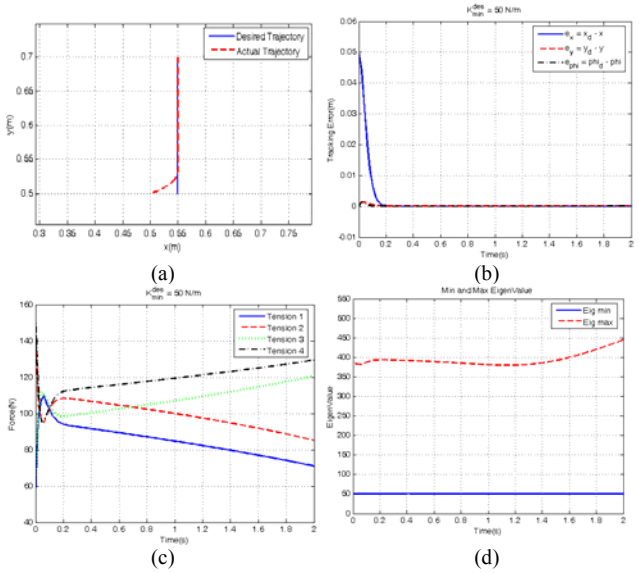

(a) (b) (c) (d)

Fig. 7. Trajectory tracking performance with LBSC: (a) the desired and actual tracking trajectories; (b) the tracking errors of x, y, ϕ; (c) the tension force in all the cables during the trajectory tracking; and (d) the evolution of the maximum and minimum eigenvalues of the stiffness matrix.

We first examined the performance of the trajectory tracking without LBSC. The desired and actual tracked trajectory is shown in Fig. 6(a). It can be seen in Fig. 6(b) that the errors converges to zero from the initial offset. Fig. 6(c) also shows that the tensions of all the cables are always positive. We then examined trajectory tracking with a desired lower bound stiffness of $\sigma_{\min}^{d} = 50\ N/m$. While tracking performance is similar as shown Fig. 7(a), the addition of the LBSC now causes the increase in the required tensions in all the cables to increase stiffness, as shown in Fig. 7(c). Fig. 7(d) depicts the maximum and minimum eigenvalues of the stiffness matrix and highlights that the minimum requirement of $50\ N/m$ is met.

B. Disturbance Rejection with/without LBSC

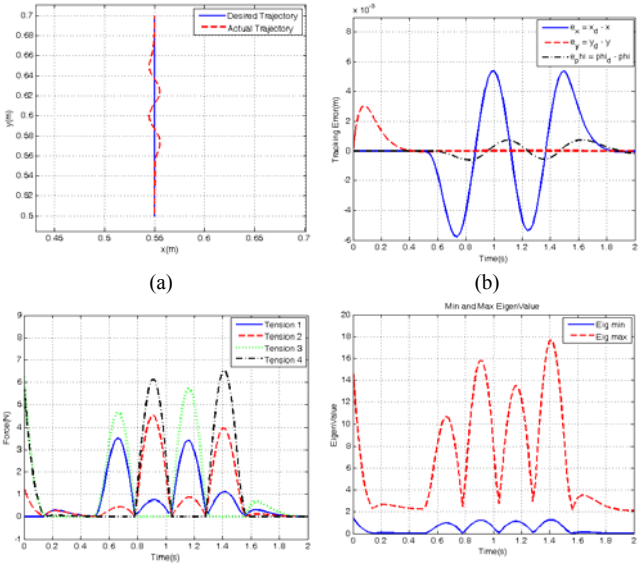

(a) (b) (c) (d)

Fig. 8. Disturbance rejection performance without LBSC: (a) the desired and actual tracking trajectories; (b) the tracking errors of x, y, ϕ; (c) the tension force in all the cables during the trajectory tracking; and (d) the evolution of the maximum and minimum eigenvalues of the stiffness matrix.

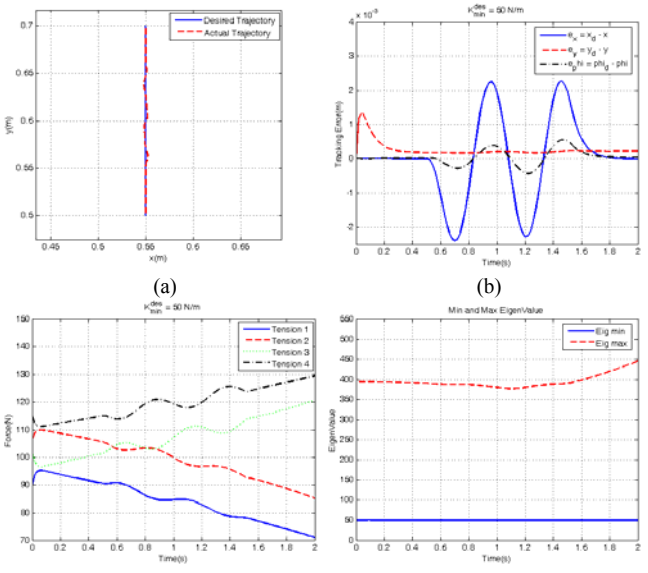

(a) (b) (c) (d)

Fig. 9. Disturbance rejection performance with LBSC: (a) the desired and actual tracking trajectories; (b) the tracking errors of x, y, ϕ; (c) the tension force in all the cables during the trajectory tracking; and (d) the evolution of the maximum and minimum eigenvalues of the stiffness matrix.

In this case study, we apply a sinusoidal disturbance forces of $F_x = 0\ N$, $F_y = 5\sin(4\pi t)\ N$ at the end-effector within the time period of $0.5\ s < t < 1.5\ s$. We again first examine its performance without LBSC. Fig. 8(a) shows the

tracking performance reflecting the deviations from the desired trajectory due the sinusoid disturbance. The maximum position error of about $6\times10^{-3}m$ can be noticed in the error plots in Fig. 8(b). The corresponding tension force profiles of cables shown in Fig. 8(c) indicates that the required forces fluctuate significantly due to the corresponding disturbance. Fig. 8(d) shows the maximum and minimum eigenvalues of the stiffness matrix, which also fluctuates according to the disturbance.

Referring to Fig. 9(a), the end-effector tracks the desired trajectory much better when the LBSC with $\sigma_{\min}^{d} = 50\ N/m$ is added. The maximum position error is $2.3\times10^{-3}m$ as shown in Fig. 9(b). The corresponding tension profiles shown in Fig. 9(c) show less fluctuations, and Fig. 9(d) also shows less fluctuation in the minimum and maximum eigenvalue of the stiffness matrix, and the minimum stiffness of $50\ N/m$ is also achieved.

VI. CONCLUSION

The actuation redundancy by virtue of the surplus cables not only provides feasible solution under the unilateral control input constraint, but also provides flexibility by way of optimal cable force distribution and task space stiffness specification and adjustment. The CCT based task space stiffness mapping provides further insights and understanding of relationship between the redundant cable actuation forces and the task stiffness. Inclusion of a lower bound task stiffness within the control scheme enable us to provide a minimal guarantee of trajectory tracking and disturbance rejection performance. The case studies with the control scheme co-simulated with a virtual prototype showed that developed method was capable of achieving the improved performance in both trajectory tracking and disturbance rejection tasks. Future works include evaluation of the proposed control scheme in a physical prototype.

REFERENCES

[1] D. Chakarov, "Study of The Antagonistic Stiffness of Parallel Manipulators with Actuation Redundancy," *Mechanism and Machine Theory,* vol. 39, pp. 583-601, 2004.

[2] J. F. O'Brien and J. T. Wen, "Redundant Actuation for Improving Kinematic Manipulability," in *IEEE International Conference on Robotics and Automation*, 1999, pp. 1520-1525.

[3] M. A. Nahon and J. Angeles, "Force optimization in redundantly-actuated closed kinematic chains," in *IEEE International Conference on Robotics and Automation*, 1989, pp. 951-956.

[4] B. J. Yi*, et al.*, "Open-loop stiffness control of overconstrained mechanisms/robotic linkage systems," in *IEEE International Conference on Robotics and Automation*, 1989, pp. 1340-1345.

[5] N. G. Dagalakis*, et al.*, "Stiffness Study of a Parallel Link Robot Crane for Shipbuilding Applications," *ASME Journal of Offshore Mechanics and Arctic Engineering,* vol. 111, pp. 183-193, 1989.

[6] R. Verhoeven*, et al.*, "Workspace, stiffness, singularities and classification of tendon-driven stewart platforms," in *6th International Symposium on Advances in Robot Kinematics*, Strobl, Austria, 1998, pp. 105-114.

[7] P. Bosscher*, et al.*, "Wrench-Feasible Workspace Generation for Cable-Driven Robots," *IEEE Transactions on Robotics,* vol. 22, pp. 890-902, October 2006.

[8] A. B. Alp, "Cable-Suspended Parallel Robots," M.S. Thesis, University of Delaware, Newark, DE, 2001.

[9] S. Behzadipour and A. Khajepour, "Stiffness of Cable-based Parallel Manipulators with Application to the Stability Analysis," *ASME Journal of Mechanical Design,* vol. 128, pp. 303-310, 2006.

[10] A. Muller, "Internal Preload Control of Redundantly Actuated Parallel Manipulators & Its Application to Backlash Avoiding Control," *IEEE Transactions on Robotics and Automation,* vol. 21, pp. 668-677, 2005.

[11] V. R. Kumar and K. J. Waldron, "Force Distribution in Closed Kinematic Chains," *IEEE Journal of Robotics and Automation,* vol. 4, pp. 657-664, December 1988.

[12] X. Yun and N. Sarkar, "Unified Formulation of Robotic Systems With Holonomic and Nonholonomic Constraints," *IEEE Transactions on Robotics and Automation,* vol. 14, pp. 640-650, 1998.

[13] S.-F. Chen and I. Kao, "Conservative Congruence Transformation for Joint and Cartesian Stiffness Matrices of Robotic Hands and Fingers," *The International Journal of Robotics Research,* vol. 19, pp. 835-847, 2000.

[14] K. Yu, "Simultaneous Trajectory Tracking and Stiffness Control of Cable Driven Parallel Manipulator," M.S., Mechanical & Aerospace Engineering, SUNY at Buffalo, Buffalo, 2007.

[15] K. Yu*, et al.*, "Simutaneous Trajectory Tracking and Stiffness Control of Cable Actuated Parallel Manipulator," in *ASME Design Engineering Technical Conferences & Computers and Information in Engineering Conference*, San Diego, CA, 2009.